Journal of Physics: Conference Series **500** (2014) 142013 doi:10.1088/1742-6596/500/14/142013

Numerical refocusing of 2d-VISAR data

David J Erskine[1], R F Smith[1], C Bolme[2], S Ali[3], P M Celliers[1] and G W Collins[1]

[1]Lawrence Livermore National Laboratory, P.O. Box 808, Livermore, CA 94551
[2]Los Alamos National Laboratory, Los Alamos, NM 87545
[3]Dept. Earth & Planetary Science, University of California, Berkeley, CA 94720

E-mail: erskine1@llnl.gov

Abstract. Two dimensional velocity interferometer (2d-VISAR) data can be treated as a kind of hologram, since fringes recorded by the interferometer manifest both phase and magnitude information about changes in the optical field of the target, over an image. By the laws of diffraction, knowledge of the optical field at one focal plane can be used to calculate the optical field at another focal plane. Hence a numerical re-focusing operation can be performed on the data post-experiment, which can bring into focus narrow features that were recorded in an out of focus configuration. Demonstration on shocked Si data is shown.

1. Introduction

An important diagnostic for shock physics over many years has been a Velocity Interferometer System for Any Reflector (VISAR) [1–4]. This measures target motion to high precision using phase shifts of fringes produced by interfering light reflected from the target at two different times, slightly delayed. Until recently, this diagnostic has been limited to measuring motion at points or lines across a target [1–3]. Recently our group introduced a two-dimensional version of a VISAR [5–10]. We have used it at the Rochester's Omega Laser system [10] and at LLNL's Jupiter Laser system [11] to measure 2d velocity and reflectivity maps. Our system has a higher spatial resolution than conventional line-VISARs, because we use optical lenses and a 4000x4000 pixel CCD detector rather than electron beam optics and a phosphor screen such as a framing camera or streak camera. But because the detector has by itself no time gating, instead of recording a time history of velocity as in a point or line-VISAR, we use pulsed illumination to freeze the target motion and measure velocity and reflectivity in a snapshot.

We report here an interesting and useful improvement to the 2d-VISAR, which is a numerical holographic post-processing (easily implemented via Fourier transform) of the complex 2d-image data which normally outputs from the VISAR analysis. If the original data was taken in an out of focus condition, we have demonstrated the ability to bring narrow features such as cracks back into focus, after the fact, when otherwise they would be blurred. This is a very useful ability, since it is often difficult to precisely focus specular targets (such as clean silicon or diamond) and anticipate their motion prior to the moment of illumination, especially with the narrow depth of field of fast lenses typically used to collect a large solid angle of light reflected from a target. This ability could also be useful for exploring the 3d debris region of a shocked textured target, or targets having 3d shape not residing in a single plane.

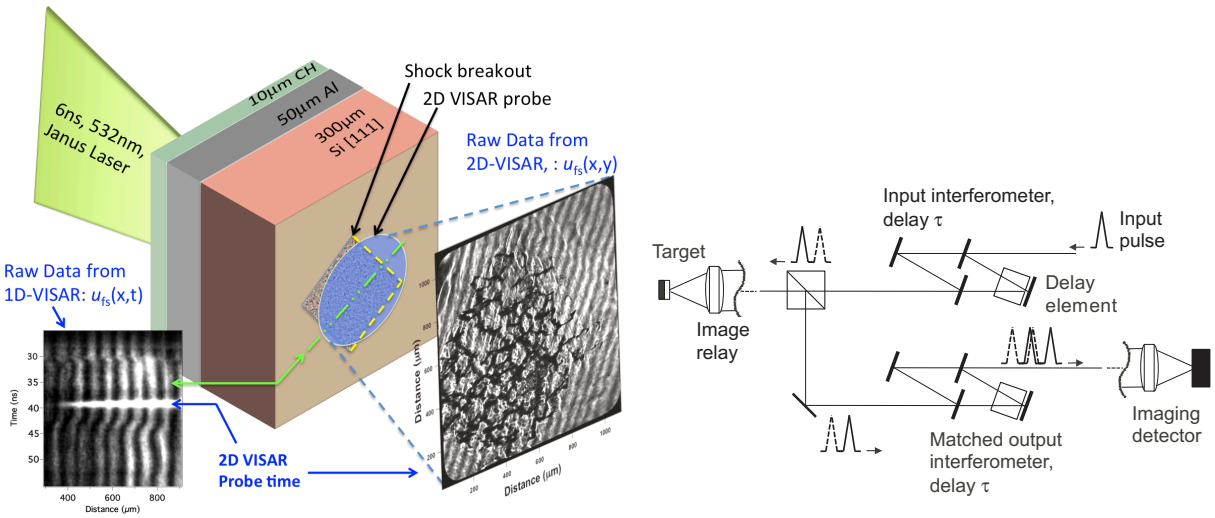

Figure 1. (Left) The 1d- and 2d velocity interferometers (VISAR) at LLNL's Jupiter Laser Facility observed the onset of fracture networks in shocked Si. The conventional 1d-VISAR lacked sufficient spatial resolution to observe the cracks but provided time history. (Right) The white light or dual interferometer velocimeter scheme [5–10] uses matched-delay illuminating and detecting interferometers to produce fringes in spite of pulsewidths (3 ps) shorter than the interferometer delay (268 ps).

However, our technique is not exactly the same as traditional holography, and a defocused (ghost) image of the target is superimposed with the focused image. Only for narrow features (which vary strongly with focus adjustment) can one approximately isolate the features.

Holography has been used previously to measure ejecta from shocked surfaces [13], and a shock front [14]. These use a conventional two beam (reference and object) arrangement to create fringes on the detector. In contrast, our technique uses a single beam, and a double pulse pair instead of a single illumination pulse. Work of Greenfield et al. [12] at LANL also uses pulsed illumination to freeze motion of a shock sample observed in 2d by an interferometer. However, their system does not record simultaneous phase quadrature, as our system does. Consequently, their spatial resolution is significantly less because they (essentially) need to use adjoining pixels to provide the phase quadrature.

We note that a 2d-VISAR operates similar to holography, since in both cases two wavefronts at optical frequency are interfered and the so-produced fringes at zero or relatively low frequency are recorded across a 2d area (image). However, the VISAR differs from conventional holography in that both of two wavefronts reflect off the target (and during that interval the target has changed slightly due to velocity or reflectivity). Whereas in a conventional holography one of the two wavefronts, called the reference wavefront, does not reflect off the target and is ideally smooth and uniform, so that features in the fringes represent just the wavefront reflected from the target.

Secondly, conventional holography can only use ultrashort pulse illumination with difficulty, because the short coherence length (∼1 mm for our 3 ps illumination) prevents fringes over a wide field, since the two paths (target & reference) are usually not colinear. Whereas in a VISAR the wavefronts overlap spatially (by use of beamsplitters) over a wide image field, provided the temporal coherence condition is satisfied. (The latter is accomplished by the use of dual-matched delay interferometers, figure 1 right).

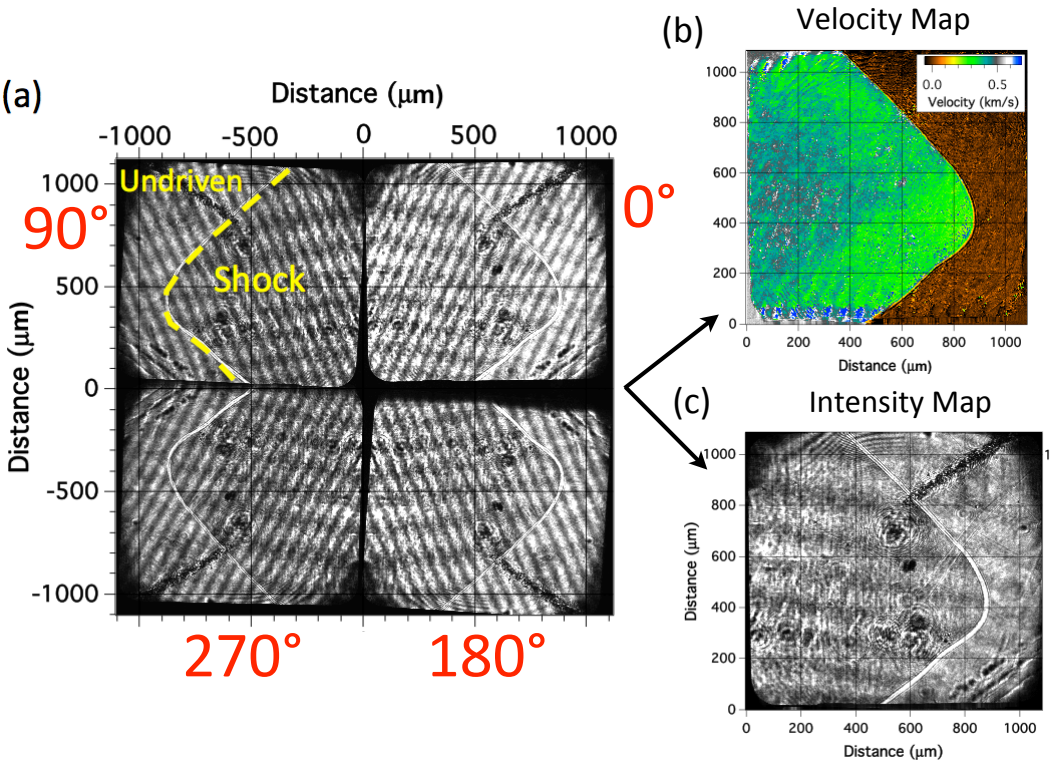

Figure 2. (a) Four simultaneous interferometer outputs having 90° phase relation are recorded on a single CCD detector chip. (b) Phase $\theta(x, y)$ and (c) nonfringing outputs. (Horizontal fringes in (c) of this shot 070910-02 are not interferometer fringes but parasitic fringes between sample and LiF window. These do not affect velocimetry result (b).)

2. Apparatus

Figure 1 (left) shows the target arrangement at the 2d-VISAR at LLNL's Jupiter Laser facility to study shocked Si [11]. A 6 ns 532 nm Janus Laser pulse hitting 10 μm of CH creates a drive pulse buffered by 50 μm of Al. The drive pulse has a square profile ~500 μm wide. The 2d VISAR optics images a ~1 mm region on the back of the Si. A line-VISAR also simultaneously measures the back of the target and provides a time history, with a spatial resolution of 30-50 μm along a 1 mm line of 15 μm width. (The moment of the snapshot 2d-VISAR exposure is recorded by a fiducial.) We are interested in the dynamics of crack formation. Unfortunately, such cracks are not sufficiently resolved by the line-VISAR which only manifests (in this case) a change in target reflectivity. Hence, the superior spatial resolution of the 2d-VISAR is crucial.

Because the CCD detector of the 2d-VISAR is integrating and has no time gating, a short pulsewidth illumination is necessary to "freeze" sample motion. The 2d-VISAR probe beam is a 3 ps 1 mJ pulse of 400 nm doubled light from a Ti-sapphire laser. The 1 mm region of target back is imaged through the detecting interferometer of the VISAR system, having a 268 ps delay between its arms. However, since the 3 ps duration of the illumination is much shorter than the detecting interferometer delay, the two wavefronts emerging from the detecting interferometer would not normally overlap in time and no interference fringes would result.

Our solution is to use a "white light" or dual matched-delay interferometer configuration [5–10] shown in figure 1 (right). This allows use of any light, incoherent or coherent, chirped pulse, or short pulsed illumination, to produce partial fringes. These have the same relation of

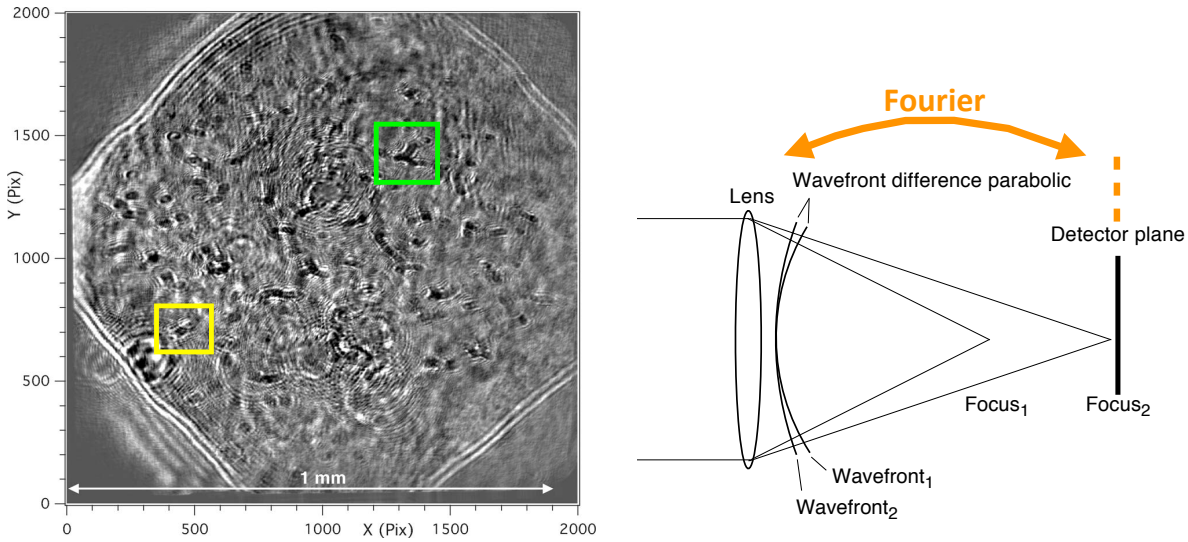

Figure 3. (Left) Nonfringing image from 2d-VISAR shot 020910-04 on Si without a window, about 1 mm field of view. Wormlike features are diffraction rings around cracks slightly out of focus. Regions in yellow and green boxes are shown as numerically focused images in figure 4. (Right) A Fourier operation transforms a wavefront between the focal and pupil planes. Adding a parabolic pupil phase difference mimics changing lens power and hence focal position.

fringe phase to target motion as in a conventional single interferometer VISAR. After passing through the first (illuminating) interferometer, a single laser pulse becomes a pair of pulses separated by delay_1. After reflecting off the target, the pair of pulses becomes four pulses by the second (detecting) interferometer having delay_2. When delay_1 and delay_2 are similar, within the coherence length of the original pulse, the inner two pulses of the outputted four overlap producing partial (50%) visibility fringes. To create a quadrature phase recording, the image is recorded four times simultaneously in four quadrants of same detector (figure 2) with 1/4 wavelength delay shift between quadrants [9, 10].

After proof of concept experiments in 1996 using incoherent white light [5, 6], a 2d-VISAR using ultrashort pulse laser illumination was successfully demonstrated at Rochester's Omega facility [9]. The 2d-VISAR at LLNL's Jupiter laser system was then modeled after that system.

3. Push-pull Data Analysis

The data analysis technique [10] for processing the four quadrants into velocity data uses push-pull math, for each pixel of the image, similar to a conventional single point push-pull VISAR [2]. On a 4000x4000 pixel CCD detector we record four 2000x2000 quadrant images of the target. The quadrants are labeled S_0, S_{90}, S_{180}, S_{270} and ideally have 90° interferometer phase stepping relationship. A simple astigmatic adjustment corrects non-ideal phase relationships [10]. For each pixel (x, y) we form two 2d outputs, nonfringing intensity (I), and complex fringing (W):

$$I = S_0 + S_{90} + S_{180} + S_{270}. \tag{1}$$

$$W = (S_0 - S_{180}) + i(S_{90} - S_{270}). \tag{2}$$

The complex fringing output is further expressed in polar coordinates and yields phase (θ) and magnitude (Mag) outputs:

$$\tan 2\pi\theta = \frac{\Im W}{\Re W}, \quad \text{Mag} = |W| \tag{3}$$

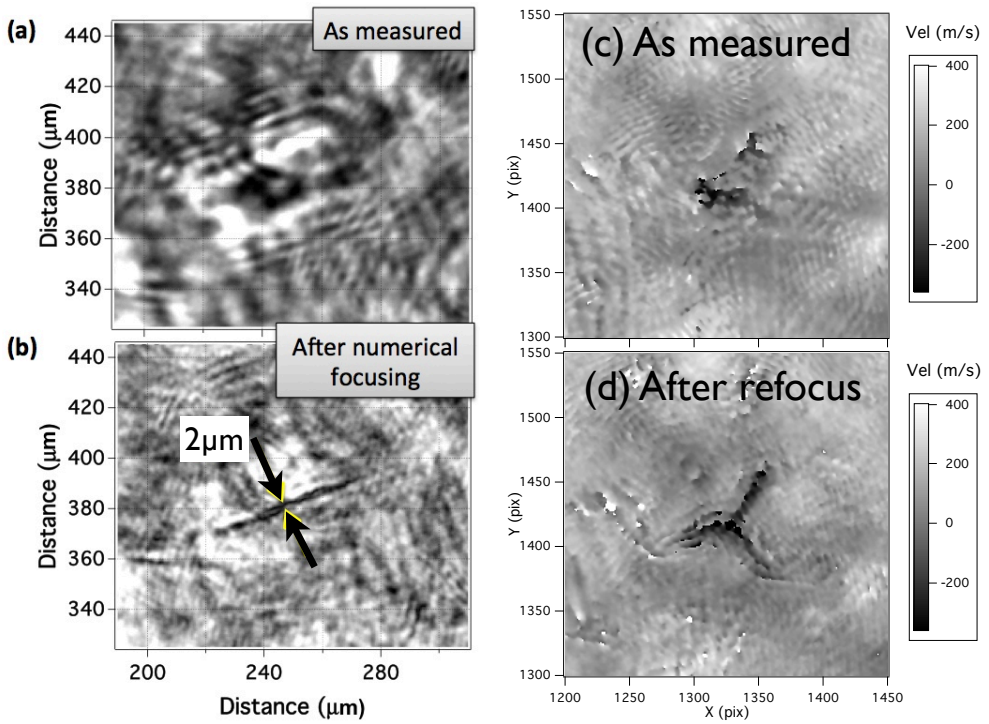

Figure 4. Before and after refocusing comparisons in shocked Si data (shot 020910-04). (a) Raw & (b) refocused magnitude $|W(x, y)|$ of feature in yellow box of figure 3. The numerically refocused crack has width of about 2 pixels, $\sim$1 μm. (c) Raw & (d) refocused velocity change ($\propto \theta$) from local average, of an interesting trigonal crack feature in green box of figure 3. Scale is 0.53 μm per pixel. The feature manifests the trigonal symmetry of Si at [111] orientation.

The magnitude $|W|$ is similar to the intensity I but without detector and incoherent light offsets. (Comparison of the two is a useful check of data validity.) The refocusing operates on W, not I, and hence the $|W(x, y)|$ and $\theta(x, y)$ are the two useful refocused outputs.

Normalized target reflectivity is obtained by dividing by $I(x, y)$ or $|W(x, y)|$ measured in a reference exposure immediately prior to the shot. Conversion from phase $\theta(x, y)$ to target velocity is by multiplication by the velocity per fringe constant (VPF), set by the interferometer delay τ as described by the equation for a conventional VISAR [15], which for our 268 ps delay is 705 m/s per fringe unwindowed.

4. Numerical Refocusing

Figure 3 is example data showing the nonfringing image from 2d-VISAR shot 020910-04 on Si without a window. The many worm-like features are cracks, slightly out of focus. These can be brought back into focus via a numerical refocusing operation: a Fourier operation transforms W from the focal plane to the pupil plane (figure 3 (left)). There a paraboloidal phase shift is applied to simulate the addition of a thin lens to shift the focal position (Z). The inverse Fourier operation is then performed, and we use outputs $|W|$ for an ordinary nonfringing image and phase $\theta(x, y)$ for velocity.

Figure 4 (right) shows example numerical focusing operation on the data, zooming on crack features shown in yellow and green boxes of figure 3. The (a) & (c) are original data recorded slightly out of focus. Note the diffraction rings in (a). The (b) & (d) are after numerical refocusing– the rings of (a) have come together to produce a narrow crack of width about 2

pixels or 1 μm. The broad features (in magnitude, phase) are not significantly changed by the refocusing operation, similar to analog refocusing. (Note that the backgrounds of (c) & (d) are similar for broad features.) Thus velocity maps already produced using out of focus data are still valid except for the very smallest scales (few microns). Numerical simulations reproduces this refocusing effect.

Space limitation prevents a full treatment here of the response of this system to a time dependent target, which will be described elsewhere. This work is preliminary, but we are excited about the possibility of exploring the three dimensional nature of the target in a way not possible with a line or point VISAR.

Acknowledgments

This work performed under the auspices of the U.S. Department of Energy by Lawrence Livermore National Laboratory under Contract DE-AC52-07NA27344.

References

[1] Barker L and Hollenbach R 1972 *J. Appl. Phys.* **43** 4669
[2] Hemsing W 1979 *Rev. Sci. Instr.* **50** 73
[3] Hemsing W, Mathews A, Warnes R, George M and Whittemore G 1992 *Shock Compression of Condensed Matter-1991* ed Schmidt S (North-Holland) 767
[4] Dolan D 2006 *Sandia National Laboratory Tech. Rep.* SAND2006-1950
[5] Erskine D and Holmes N 1995 *Nature* **377** 317
[6] Erskine D J and Holmes N C 1997 Imaging White Light VISAR *SPIE Proc. Ser.* **2869** 1080
[7] Erskine D 1997 *US Patent* **5,642,194**
[8] Erskine D 2000 *US Patent* **6,115,121**
[9] Celliers P M, Erskine D J, Sorce C M, Braun D G, Landen O L and Collins G W 2010 *Rev. Sci. Instrum.* **81** 035101
[10] Erskine D J, Smith R F, Bolme C A, Celliers P M and Collins G W 2012 *Rev. Sci. Instrum.* **83** 043116
[11] Smith R, Bolme C, Erskine D, Celliers P, Ali S, Eggert J, Brygoo S, Hammel B, Wang J and Collins G 2013 *J. Appl. Phys.* **114** 133504
[12] Greenfield S R, Luo S N, Paisley D L, Loomis E N, Swift D C and Koskelo A C 2007 *AIP Conf. Proc.* **955** 1093
[13] McMillan C F and Whipkey R K 1989 Holographic measurement of ejecta from shocked metal surfaces *SPIE Proc. Ser.* **1032** 553
[14] Watanabe M, Abe A, Casey R T and Takayama K 1992 Holographic interferometric observation of shock wave phenomena *SPIE Proc. Ser.* **1553** 418
[15] Barker L and Schuler K 1974 *J. Appl. Phys.* **45** 3692